Natural Resources Canada
Ressources naturelles Canada

Preliminary results of geology of the Portage deposit, Meadowbank gold mine, Churchill Province, Nunavut

V. Janvier, S. Castonguay, P. Mercier-Langevin, B. Dubé, V. McNicoll, S. Pehrsson, M. Malo, B. De Chavigny, and O. Côté-Mantha

Geological Survey of Canada
Current Research 2015-2

2015

Canada

Geological Survey of Canada
Current Research 2015-2

Preliminary results of geology of the Portage deposit, Meadowbank gold mine, Churchill Province, Nunavut

V. Janvier, S. Castonguay, P. Mercier-Langevin, B. Dubé, V. McNicoll, S. Pehrsson, M. Malo, B. De Chavigny, and O. Côté-Mantha

2015

ISSN 1701-4387
Catalogue No. M44-2015/2E-PDF
ISBN 978-1-100-25355-8
doi:10.4095/295532

A copy of this publication is also available for reference in depository libraries across Canada through access to the Depository Services Program's Web site at http://dsp-psd.pwgsc.gc.ca

This publication is available for free download through GEOSCAN
http://geoscan.ess.nrcan.gc.ca

Recommended citation

Janvier, V., Castonguay, S., Mercier-Langevin, P., Dubé, B., McNicoll, V., Pehrsson, S., Malo, M., De Chavigny, B., and Côté-Mantha, O., 2015. Preliminary results of geology of the Portage deposit, Meadowbank gold mine, Churchill Province, Nunavut; Geological Survey of Canada, Current Research 2015-2, 18 p. doi:10.4095/295532

Critical review

N. Pinet

Authors

V. Janvier(Vivien.Janvier@ete.inrs.ca)
M. Malo(michel.malo@ete.inrs.ca)
Institut National de la Recherche Scientifique
Centre Eau-Terre-Environnement
490, rue de la couronne
Québec, Quebec G1K 9A9

S. Castonguay
(Sebastien.Castonguay@RNCan-NRCan.gc.ca)
P. Mercier-Langevin
(Patrick.Mercier-Langevin@RNCan-NRCan.gc.ca)
B. Dubé
(Benoit.Dube@RNCan-NRCan.gc.ca)
Geological Survey of Canada
490, rue de la couronne
Québec, Quebec G1K 9A9

V. McNicoll (Vicki.McNicoll@NRCan-RNCan.gc.ca)
S. Pehrsson (Sally.Pehrsson@NRCan-RNCan.gc.ca)
Geological Survey of Canada
601 Booth Street
Ottawa, Ontario K1A 0E8

B. De Chavigny (Benoit.DeChavigny@agnicoeagle.com)
Agnico Eagle Mines Ltd.
Meadowbank Division, Baker Lake
Nunavut X0C 0A0

O. Côté-Mantha (olivier.cote-mantha@agnicoeagle.com)
Agnico Eagle Mines Ltd.
Exploration Division
C.P. 87-765, chemin de la mine Goldex
Val d'Or, Quebec J9P 4N9

Correction date:

Preliminary results of geology of the Portage deposit, Meadowbank gold mine, Churchill Province, Nunavut

V. Janvier, S. Castonguay, P. Mercier-Langevin, B. Dubé, V. McNicoll, S. Pehrsson, M. Malo, B. De Chavigny, and O. Côté-Mantha

Janvier, V., Castonguay, S., Mercier-Langevin, P., Dubé, B., McNicoll, V., Pehrsson, S., Malo, M., De Chavigny, B., and Côté-Mantha, O., 2015. Preliminary results of geology of the Portage deposit, Meadowbank gold mine, Churchill Province, Nunavut; Geological Survey of Canada, Current Research 2015-2, 18 p. doi:10.4095/295532

Abstract: The Meadowbank banded iron-formation–hosted world-class gold deposit is comprised in the polydeformed and metamorphosed 2711 Ma Pipedream-Third Portage sequence of the Woodburn Lake Group, which also comprises mafic and ultramafic rocks, and quartzite. At least four phases of regional Trans-Hudsonian (Proterozoic) deformation are documented in the Meadowbank deposit area: 1) isoclinal F_{P1} folds and D_{P1} fault zones, strongly overprinted by younger deformation; 2) north-trending isoclinal F_{P2} folds and associated D_{P2} fault zones cutting the stratigraphy and mineralization; and two set of younger folds, 3) open to closed southwest-plunging F_{P3} folds, and 4) shallowly to moderately inclined, open to tight, chevron-style mesoscopic F_{P4} folds. The bulk of the gold at Meadowbank is hosted in banded iron-formation and occurs at or near the contact with sheared ultramafic rocks where it is associated with pyrrhotite±pyrite and traces of chalcopyrite and arsenopyrite. Gold-rich quartz-pyrrhotite±pyrite veins are locally present in intermediate to felsic volcaniclastic rocks interlayered with banded iron-formation units. The ore-associated mineral assemblages include grunerite and/or cummingtonite and chlorite in banded iron-formation layers, whereas sericite±chlorite dominate in altered volcaniclastic rocks. Geochemical analyses of the major rock types are essential to further discriminate the host units, thus increasing the knowledge of the stratigraphic and structural setting of the deposit. Crosscutting relationships indicate that the bulk of the gold was introduced prior to D_{P2}, preferentially near or along fault zones developed at contacts between banded iron-formation units and ultramafic rocks.

Résumé : Le gisement aurifère de classe mondiale de Meadowbank, encaissé dans une formation de fer rubanée, est contenu dans la séquence polydéformée et métamorphisée datant de 2711 Ma de Pipedream-Third Portage du Groupe de Woodburn Lake, qui comprend également des roches mafiques et ultramafiques, ainsi que du quartzite. Au moins quatre phases de la déformation régionale trans-hudsonienne (Protérozoïque) sont documentées dans la région du gisement de Meadowbank : 1) plis isoclinaux P_{P1} et zones de failles D_{P1} avec forte surimpression d'une déformation plus récente; 2) plis isoclinaux P_{P2} de direction nord auxquels sont associées des zones de failles D_{P2} recoupant la stratigraphie et la minéralisation; et deux ensembles de plis plus récents; 3) plis P_{P3} ouverts à serrés plongeant vers le sud-ouest; et 4) plis mésoscopiques P_{P4} en chevrons, ouverts à serrés, faiblement à modérément déjetés. La majeure partie de l'or au gisement de Meadowbank est encaissée dans une formation de fer rubanée et se présente au contact ou près du contact avec des roches ultramafiques cisaillées où elle est associée à de la pyrrhotite±pyrite et des traces de chalcopyrite et d'arsénopyrite. Des filons de quartz-pyrrhotite±pyrite riches en or sont présents par endroits dans des roches volcanoclastiques intermédiaires à felsiques interstratifiées avec les formations de fer rubanées. Les associations minérales de la zone minéralisée comprennent de la grunérite ou de la cummingtonite et de la chlorite dans les horizons de formation de fer rubanée, alors que la séricite±chlorite est dominante dans les roches volcanoclastiques altérées. Des analyses géochimiques des principaux types de roche sont essentielles pour mieux différencier les unités encaissantes, de façon à améliorer notre compréhension du cadre stratigraphique et structural du gisement. Les relations de recoupement indiquent que la mise en place de la majeure partie de l'or a eu lieu antérieurement à D_{P2}, principalement à proximité ou le long de zones de failles qui se sont formées aux contacts entre des formations de fer rubanées et des roches ultramafiques.

INTRODUCTION

The Meadowbank mine, owned and operated by Agnico Eagle Mines Ltd., is located in the Kivallik region of Nunavut, approximately 70 km north of the community of Baker Lake (Fig. 1). The Meadowbank deposit, mined since 2010, is a world-class Precambrian banded iron-formation–hosted gold deposit. It constitutes one of the best examples of such deposit type and an opportunity for studying the geological and hydrothermal footprints of banded iron-formation–hosted gold deposits and the key structural controls on gold mineralization. The Meadowbank mine contains a total of about 4.2 million ounces (119.07 t) of gold, including 1.3 million ounces (36.854 t) produced from 2010 to 2013, 1.8 million ounces (51.029 t) in reserve and 1.2 million ounces in (34.019 t) resources comprised in the Portage, Goose, and Vault deposits (as of December 31, 2013; www.agnicoeagle.com; [accessed September 16, 2014]). The bulk of the gold is hosted in banded magnetite-chert iron-formation units, but a significant amount of gold is also associated with quartz veins in the intercalated intermediate to felsic volcaniclastic rocks. The mineralized succession is part of the polydeformed and metamorphosed 2711 Ma Pipedream-Third Portage sequence of the Woodburn Lake Group (Sherlock et al., 2004).

In the Meadowbank mine area, the Woodburn Lake Group comprises several major banded iron-formation units, including the East banded iron-formation, the Central banded iron-formation and the West banded iron-formation (Fig. 2). Despite their similarity (e.g. Gourcerol et al., 2014), only the Central banded iron-formation contains economic gold concentration (Portage and Goose deposits), suggesting that key ore-forming processes and elements were only active or present in that very specific area. Establishing the key ore-forming events at Meadowbank mine could have a major impact on exploration models as well as on genetic models for banded iron-formation–hosted gold deposits.

Previously published research on the Meadowbank mine area by Armitage and James (1991), Armitage et al. (1996), Sherlock et al. (2001a, 2004), Hrabi et al. (2003), and Pehrsson et al. (2013) were mainly concerned with the regional geological and hydrothermal characteristics of the deposit based on surface and trench mapping, and limited exploration drillholes, i.e. prior to any mining operation. As such, key knowledge on the tridimensional geometry of the deposit, the geochemistry of host rocks, and structural controls of mineralization has been limited. Access to the mine workings, exploration and delineation drill core, and mining data provides a wealth of new information that allows for an in depth characterization of the deposit. The current research, which includes a doctoral research project by the senior author, V. Janvier, is conducted under the auspices of Lode Gold Project of the Targeted Geoscience Initiative 4 Program (Dubé et al., 2011). The present authors' field-based research completed thus far comprises the geological mapping of the deposit, including detailed description of several drillhole sections and thorough geochemical characterization of host rocks and their alteration (Castonguay et al., 2012, 2013; Janvier et al., 2013). In addition, fieldwork was undertaken to bridge the gap between deposit-scale and regional-scale knowledge, which included sampling for geochronology of key units in and around the deposit (Castonguay et al., 2013) and a study of the Vault gold deposit 10 km north of Portage and Goose deposits (Dupuis et al., 2014). The present report aims to summarize the preliminary observations and results of the main geological features of the Portage deposit with an emphasis on the chemical signature of host rocks, on the geometry of the deposit and its structural controls, and on the ore and associated mineral assemblages.

GEOLOGICAL SETTING

The Meadowbank deposit is hosted in Pipedream-Third Portage sequence of the Woodburn Lake Group, in the Rae Domain of the western Churchill Province (Fig. 1a). The Rae Domain is dominated by Mesoarchean to Neoarchean granodioritic-tonalitic orthogneiss and volcanosedimentary rocks (Hoffman, 1989; Zaleski et al., 1997, 1999b; Skulski et al., 2003; Berman et al., 2005). The Woodburn Lake Group constitutes part of a greenstone belt that extends for over 1500 km (Fig. 1a). It includes ultramafic to mafic volcanic rocks, intermediate volcanic rocks, banded iron-formation units, quartzite, and oligomictic conglomerate, metamorphosed to greenschist to amphibolitic facies (Henderson et al., 1991; Zaleski et al., 1997). This succession of rocks is generally considered to have been deposited during the intracratonic rifting of the Mesoarchean basement (Ashton, 1988; Zaleski et al., 2001). The Woodburn Lake Group is subdivided into five sequences (Pehrsson et al., 2013; Fig. 1b): The Meadowbank deposit is comprised in the Pipedream-Third Portage sequence. The Woodburn Lake Group is overlain by the Paleoproterozoic sedimentary rocks comprising the Ketyet River Group.

The rock units of the Woodburn Lake Group in the Meadowbank mine area have been deformed during Archean orogenic events, but mainly throughout the Proterozoic Trans-Hudsonian Orogeny (Ashton, 1988; Zaleski et al., 1999a; Zaleski and Pehrsson, 2005; Berman et al., 2005, 2007). Archean fabrics are mainly cryptic in the Meadowbank area, however, at least four Proterozoic phases of deformation have been regionally described (Hrabi et al., 2003; Sherlock et al., 2004; Pehrsson et al., 2004, 2013; Fig. 2). The first two Proterozoic deformation episodes (D_{P1} and D_{P2}) consist of tight to isoclinal folds. In areas less affected by younger deformation, the regional vergence of F_{P1} and F_{P2} folds are respectively to the south and northwest. In areas of strong D_{P2} strain or along long limbs of F_{P2} folds, the S_{P1} and S_{P2} axial-planar schistosities become generally coplanar, thus difficult to differentiate and are often described as a composite S_{P1-2} fabric. Fault zones associated with these two major episodes of deformation have an impact on the distribution and geometry of ore zones, which will be discussed

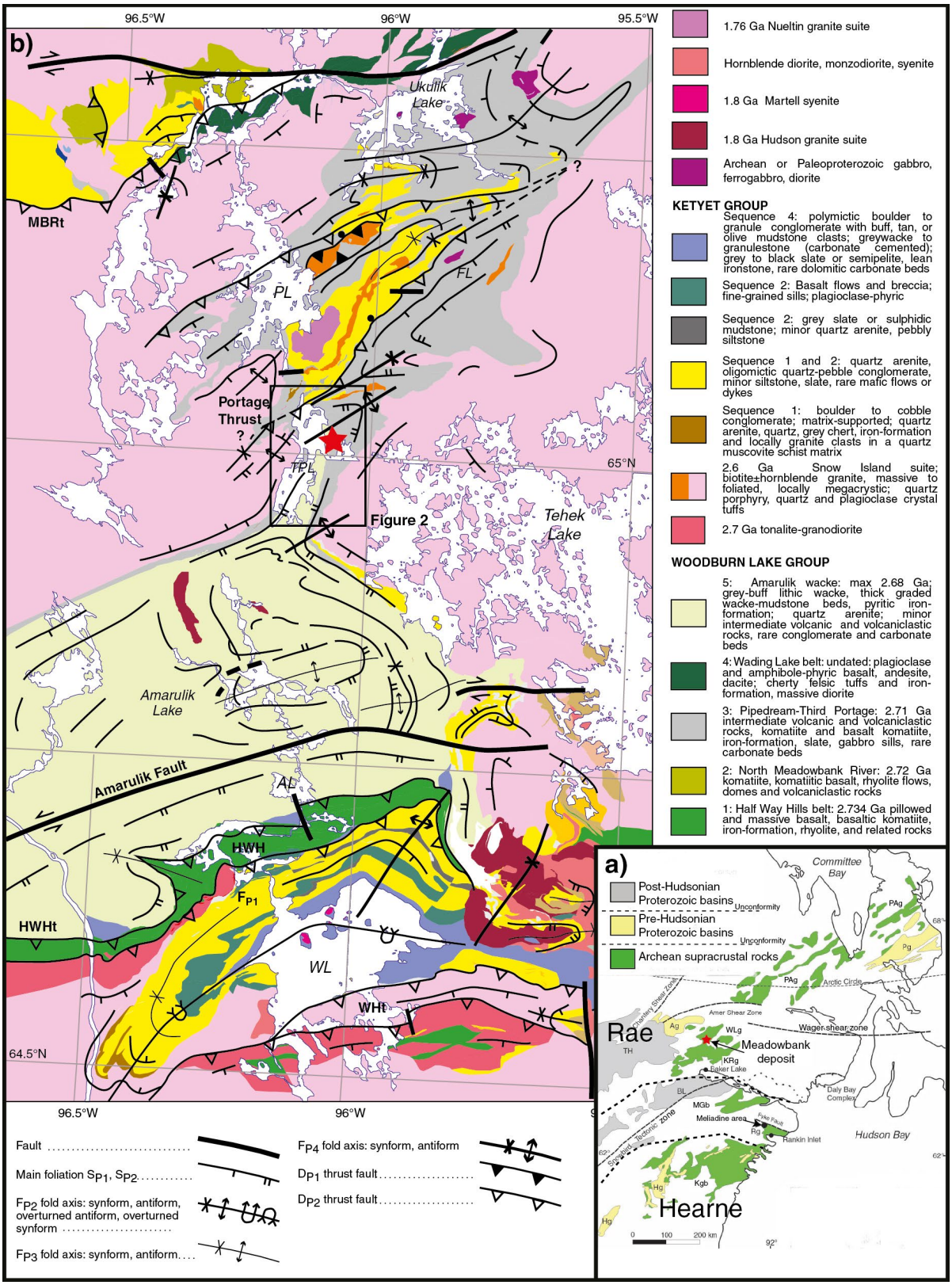

Figure 1. a) Simplified geology of the western Churchill Province (*modified from* Hrabi et al., 2003). **b)** Geology of the Woodburn Lake area and principal structural features (map and structural nomenclature *modified from* Pehrsson et al., 2013). AL = Amarulik Lake, FL = Farside Lake, HWH = Halfway Hills belt, HWHt = Halfway Hills thrust, MBRt = Meadowbank River thrust, PL = Pipedream Lake, TL = Tehek Lake, TPL = Third Portage Lake, UL = Ukulik Lake, WL = Whitehills Lake, WHt = Whitehills thrust.

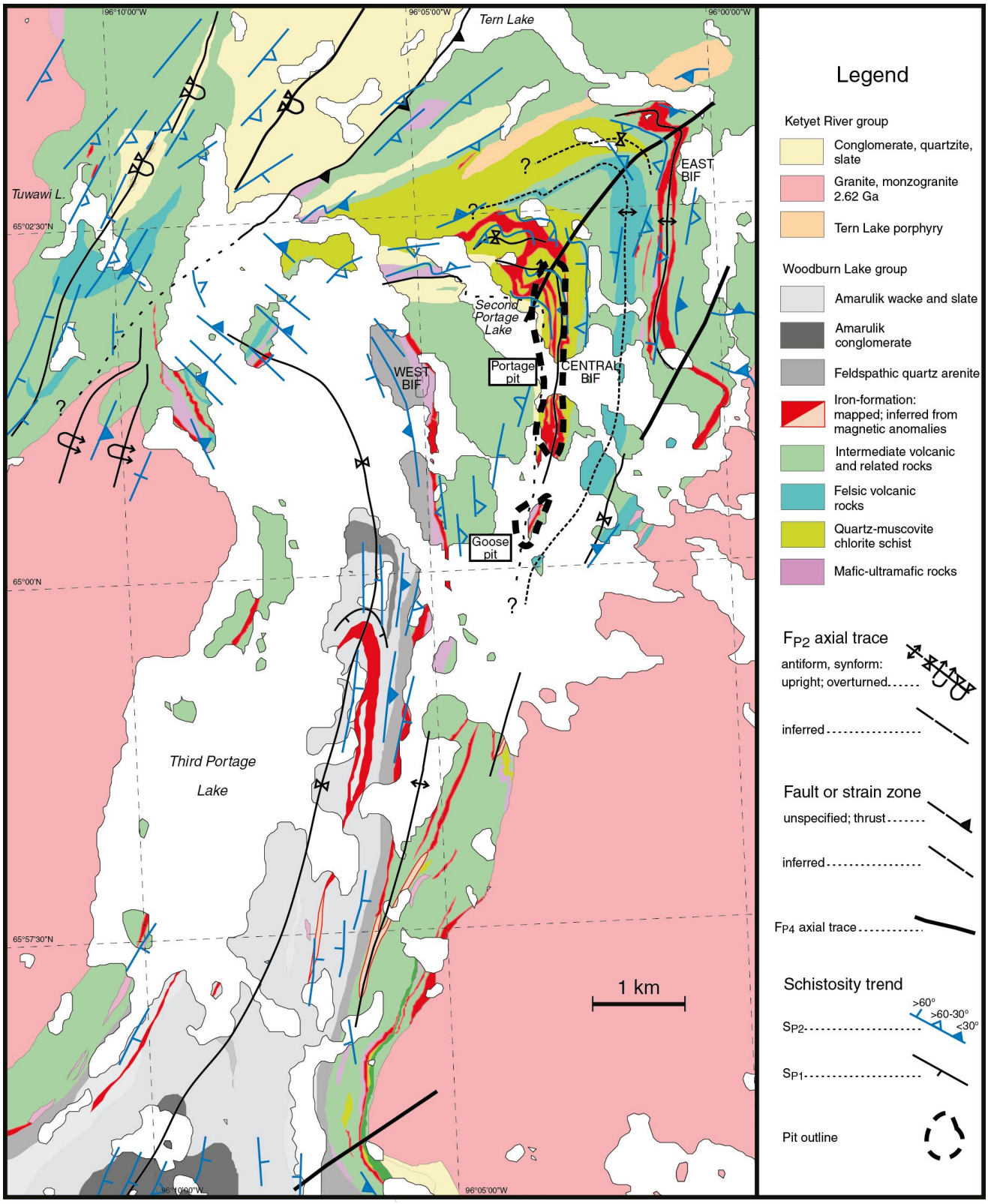

Figure 2. Geology and structure of the Meadowbank gold deposit area (map and structural nomenclature *modified from* Pehrsson et al., 2013). BIF = banded iron-formation

below. The third Proterozoic deformation (D_{P3}) comprises shallowly to moderately north- to northwest-inclined, open to tight chevron-style mesoscopic folds, locally marked by an axial-planar S_{P3} crenulation cleavage. The D_{P4} regional deformation consist of megascopic upright southwest- or northeast-plunging chevron folds.

HOST ROCK UNITS

The Meadowbank deposit comprises several altered, intensely deformed and metamorphosed rock. These units are often difficult to differentiate visually, and lithogeochemistry was used for deposit-scale mapping. From east to west, they consist of intermediate volcaniclastic rocks (unit 1), banded iron-formation units intercalated with intermediate to felsic (unit 2) and felsic (unit 3) volcaniclastic rocks, mafic rocks (unit 4), ultramafic rocks (unit 5), quartzite with mafic (unit 6) and intermediate volcanic interlayers (unit 7; Sherlock et al., 2001b; Fig. 3, 4). Intermediate dykes (unit 8) are also present on the west wall of open pit E (Fig. 3a). Unit 1 consists of massive beds of intermediate volcaniclastic rocks that form the structural footwall of the ore. It is generally quartz- and plagioclase-phyric with a groundmass of fine-grained quartz, plagioclase, and biotite. The intermediate to felsic volcaniclastic rocks of unit 2, which are commonly intercalated with banded iron-formation, are medium to fine grained and composed mainly of quartz±plagioclase with variable amount of chlorite and sericite. Unit 2 comprises medium- to fine-grained intermediate to felsic volcanoclastic rocks, commonly intercalated with banded iron-formation, and composed mainly of quartz±plagioclase with significant amount of muscovite and chlorite. Quartz veinlets are common in unit 2. Unit 3 is a felsic volcaniclastic rock, commonly muscovite-altered and intensely foliated, forming distinct muscovite schist. The banded iron-formation units consist of millimetre- to centimeter-scale magnetite and chert layers (1 mm to 3 cm) with variable amounts of grunerite and/or cummingtonite, chlorite, greenalite, and stilpnomelane. The auriferous iron–formation units contain significant amounts of pyrrhotite, pyrite, and arsenopyrite with some chalcopyrite. The ultramafic and mafic rocks (units 4 and 5) are generally located in the structural hanging wall of the ore zones. It is still not clear whether these two units are distinct lithologies or if they represent alteration end-members of a single unit. The ultramafic rocks of unit 5 are characterized by an assemblage of chlorite, talc±amphibole, and contain abundant quartz-carbonate veins and veinlets. Massive, coarse-grained, amphibole-rich rocks are common near the lower contact of the ultramafic unit. The mafic rocks of unit 4 generally differ from the ultramafic rocks by a more massive, less schistose aspect and by the absence of quartz-carbonate veinlets. A massive quartzite, including a basal polymictic conglomerate, structurally overlies the deposit host succession (Fig. 3). Minor mafic (unit 6) and intermediate (unit 7) volcanic rocks, respectively, consisting of chlorite and biotite schist units, occur as conspicuous layers within the quartzite.

GEOCHEMISTRY: CHARACTERIZATION OF PROTOLITHS

Sampling of the different units for lithogeochemistry was done along six representative vertical drill sections (N4800, N5775, N6100, N6175, N7025, N7500) across the deposit. Targeted sampling was done in the open pit to further constrain the distribution of some units and alteration assemblages. Major, trace, and rare-earth element (REE) ICP-MS analyses have been systematically carried out on a suite of volcanic rock samples. All rock units in the vicinity of the mineralized zone are strongly altered and their primary geochemical signatures are commonly significantly obscured, especially for mobile elements. The major variations of SiO_2 content shown on a SiO_2 versus Zr/TiO_2 diagram (Winchester and Floyd, 1977) attest to the strong alteration of all rock units (Fig. 5a). Although visual recognition of the different rock units allows for a preliminary classification, the use of lithogeochemical data, and more specifically ‘immobile’ or ‘least mobile’ elements such as Zr, Ti, Al, Y, Cr, Ni, Sc, V, and REEs, is essential to further differentiate the subtle variations, characterize distinct protoliths, and thus identify mappable units.

Dominant rock types

The Zr/TiO_2 versus Al_2O_3/TiO_2 binary diagram is useful to discriminate four major groups of volcanic rocks: intermediate volcaniclastic rocks (unit 1), intermediate to felsic volcaniclastic rocks (unit 2), mafic rocks (unit 4), and ultramafic rocks (unit 5; Fig. 5b).

The intermediate volcaniclastic rocks are characterized by Zr/TiO_2 ratios that are generally lower than 0.025 (Fig. 5b), an andesitic composition (Fig. 5c), and a calc-alkaline magmatic affinity (Fig. 5d). Chondrite-normalized trace and rare-earth elements of the intermediate unit show an arc-style signature with negative Nb, Ta, and Ti anomalies (Fig. 6a). The intermediate rocks of unit 1 can be separated in three subunits, 1a, 1b, and 1c. The subunits 1a and 1b have Al_2O_3/TiO_2 ratios that are generally higher than 18, whereas unit 1c has ratios that are generally lower than 18. Subunits 1a and 1b can be differentiated using a chondrite-normalized trace and rare-earth element plot, subunit 1b being characterized by slightly lower Th and HREE values than subunit 1a (Fig. 6a). Subunit 1a generally lies at the base of the mine host succession, whereas subunit 1b always occurs at the top, above the WD_{P2} fault zone (Fig. 7a). Subunit 1c, which is characterized by negative Zr-Hf anomalies, higher light-REE values, is only present in the northern

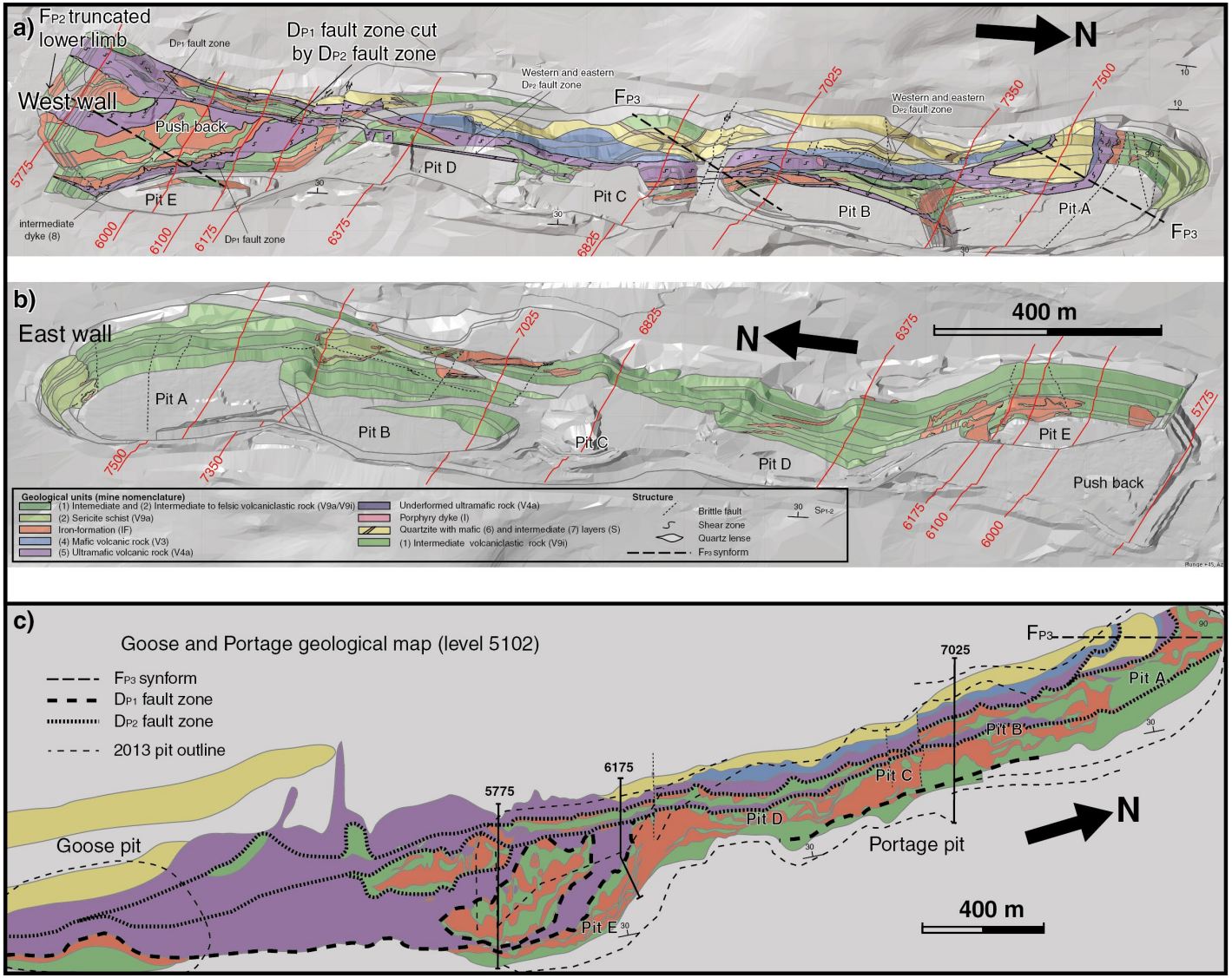

Figure 3. Oblique views of the geology of the **a)** western wall and **b)** eastern wall of the Portage pit, Meadowbank deposit; **c)** geological map of the Meadowbank deposit at level 5102 m. Mine-scale structural nomenclature is used.

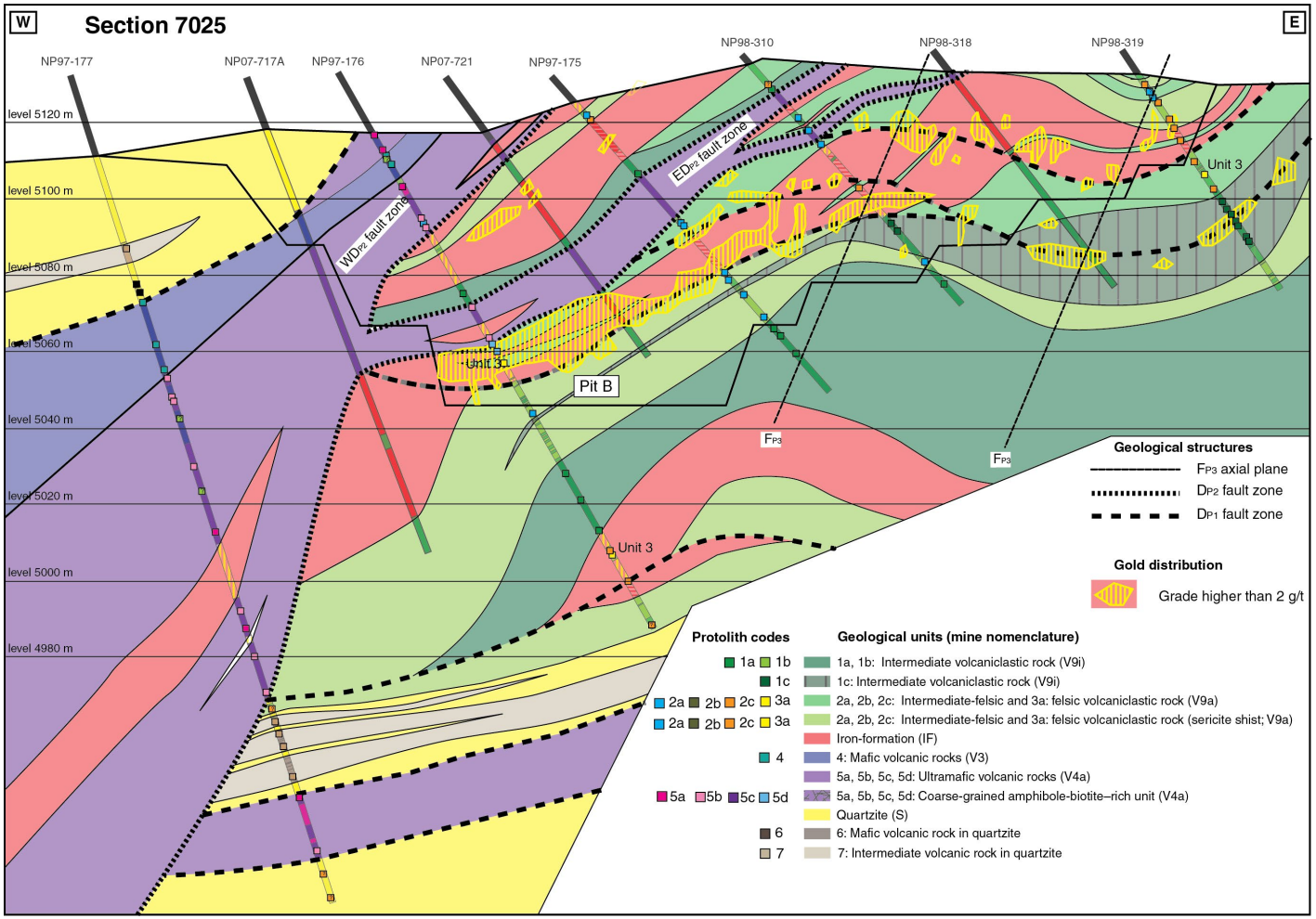

Figure 4. Interpreted geological section N7025 of Meadowbank deposit showing the complex fault imbrications and the distribution of gold. Mine-scale structural nomenclature is used.

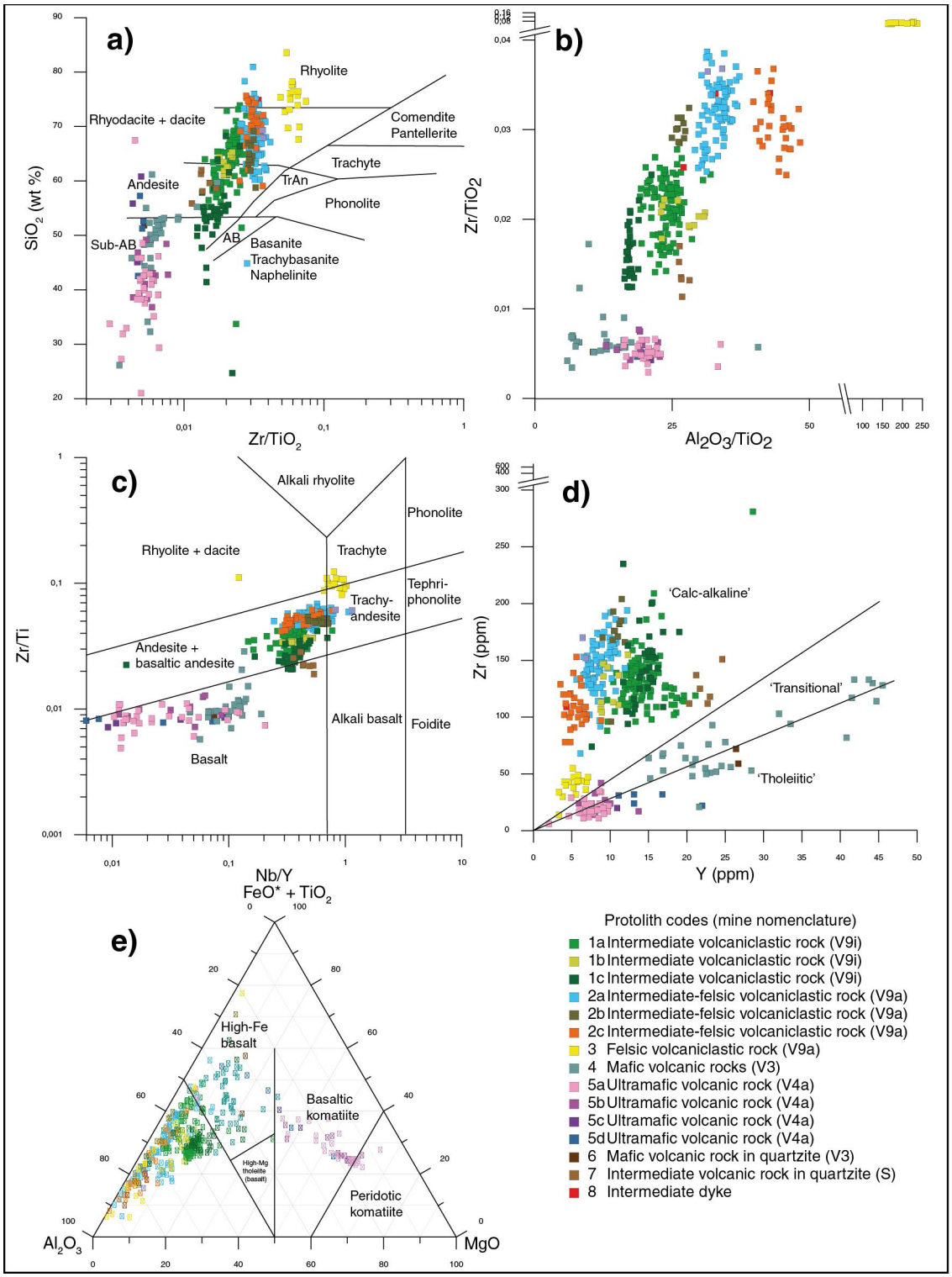

Figure 5. Geochemical discrimination diagrams for the volcanic and volcaniclastic rocks of the Meadowbank deposit area; **a)** SiO_2 versus Zr/TiO_2 classification diagram (Winchester and Floyd 1977), **b)** Zr/TiO_2 versus Al_2O_3/TiO_2 ratio diagram, **c)** Zr/Ti versus Nb/Y classification diagram (Winchester and Floyd 1977), **d)** Zr versus Y magmatic affinity diagram from Barrett and MacLean (1999), and **e)** AFM ternary diagram from Jensen (1976). AB = andesitic basalt, TrAn = trachyandesite

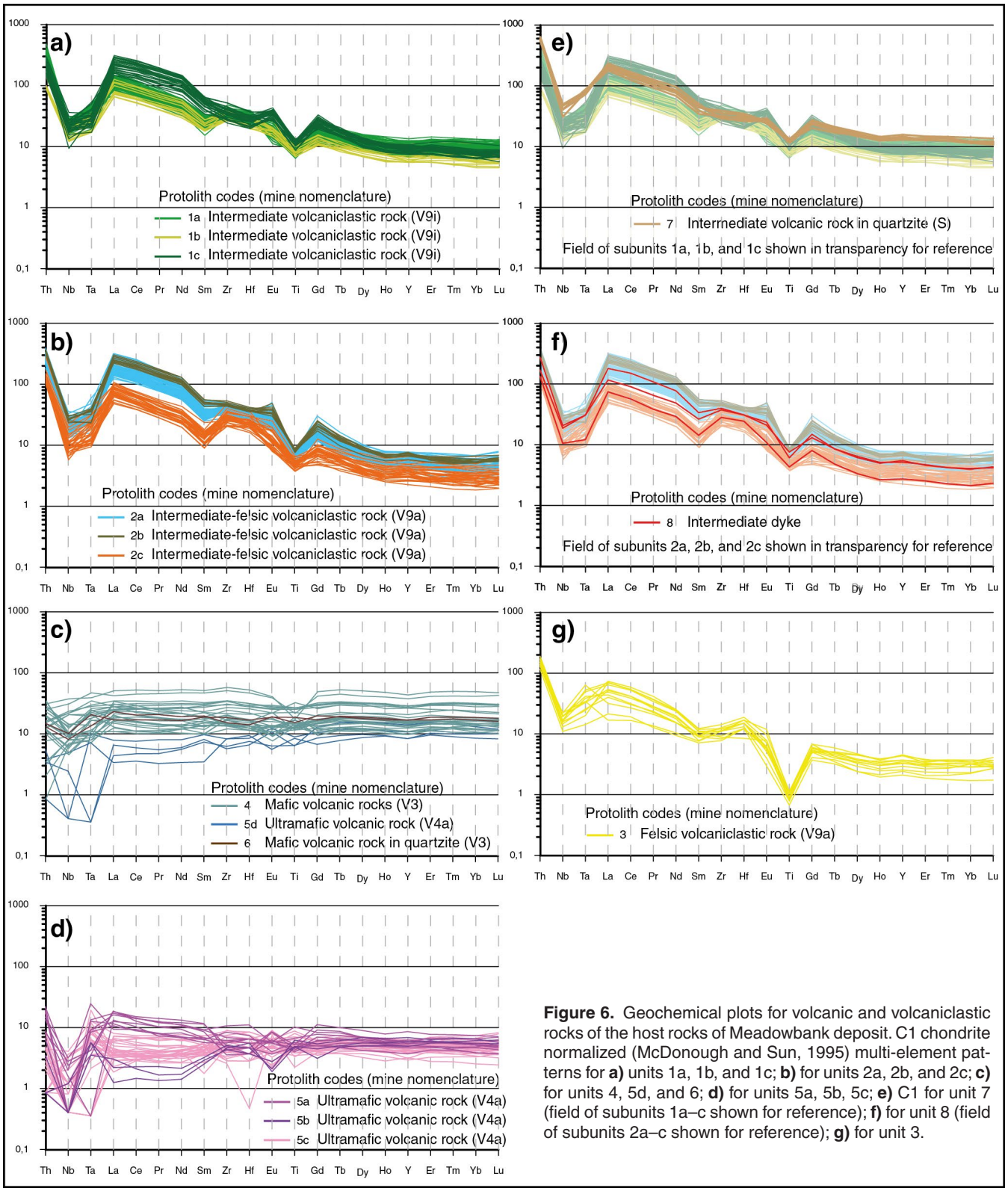

Figure 6. Geochemical plots for volcanic and volcaniclastic rocks of the host rocks of Meadowbank deposit. C1 chondrite normalized (McDonough and Sun, 1995) multi-element patterns for **a)** units 1a, 1b, and 1c; **b)** for units 2a, 2b, and 2c; **c)** for units 4, 5d, and 6; **d)** for units 5a, 5b, 5c; **e)** C1 for unit 7 (field of subunits 1a–c shown for reference); **f)** for unit 8 (field of subunits 2a–c shown for reference); **g)** for unit 3.

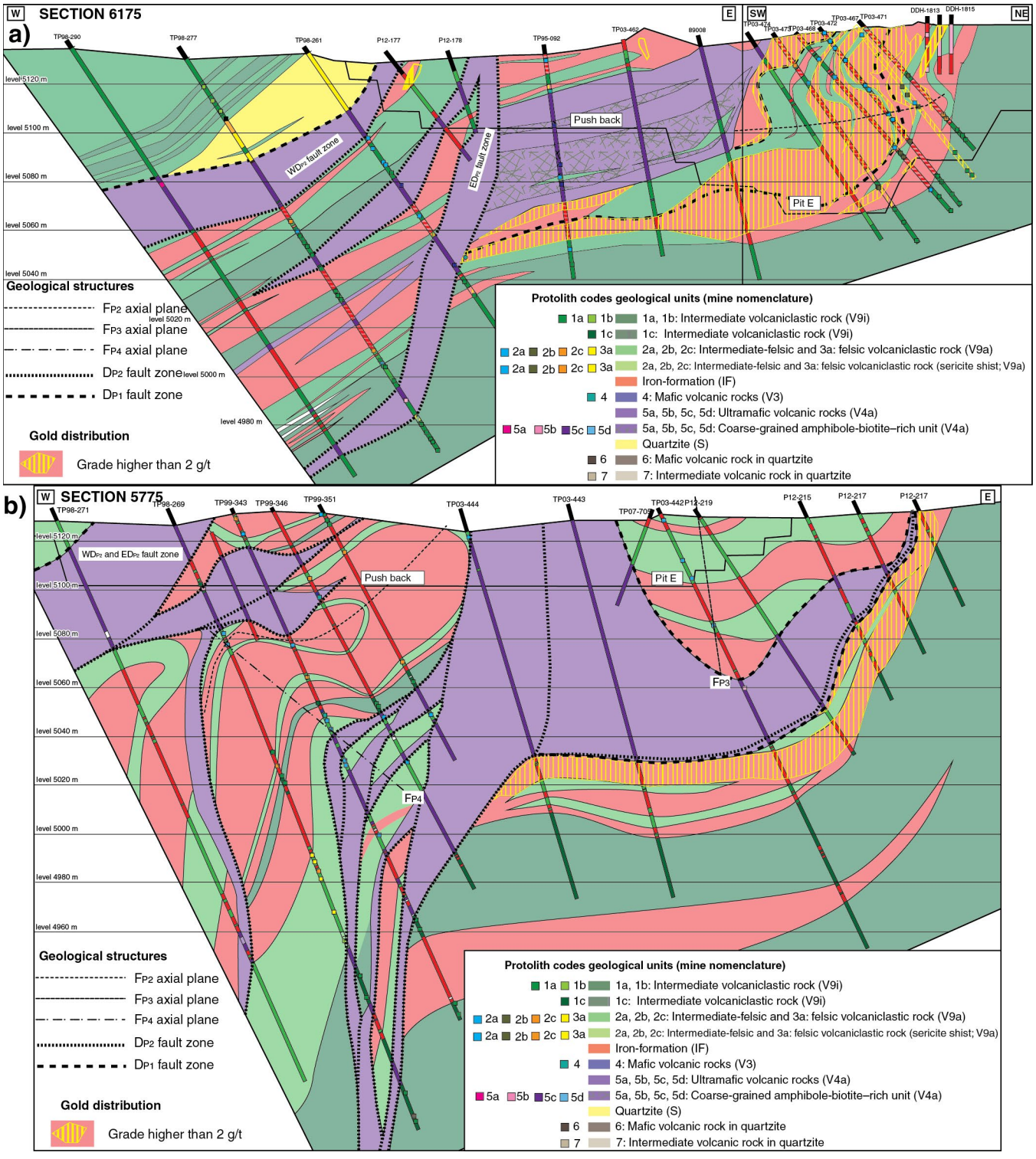

Figure 7. Interpreted geological section **a)** N5775 and **b)** N6175, showing the polyphase structure events and the distribution of gold. Mine-scale structural nomenclature is used.

part of the Portage deposit (e.g. section N7025), structurally above subunit 1a and interlayered with intermediate to felsic volcaniclastic rocks of unit 2 (Fig. 4).

The intermediate to felsic volcaniclastic rocks of unit 2 can also be divided in three subunits on the basis of the chemistry: subunits 2a, 2b, and 2c have Zr/TiO_2 ratios that are generally higher than 0.025, distinctive Al_2O_3/TiO_2 ratios (Fig. 5b), an andesitic to dacitic composition (Fig. 5c), and a calc-alkaline magmatic affinity (Fig. 5d). Chondrite-normalized trace and rare-earth element plots show that these subunits have an arc-style signature with negative Nb, Ta, and Ti and that they are depleted in HREEs compared to the intermediate rocks (i.e. unit 1; Fig. 6b). Subunits 2a and 2b show similar patterns, are enriched in LREEs compared to subunit 2c, and unlike subunit 1c, do not have positive Zr-Hf anomalies (Fig. 6b). Subunit 2b can be differentiated from subunit 2a by its higher content in Th. In section 6175 (Fig. 7a), subunit 2b is structurally above subunit 2a.

The mafic rocks (unit 4) have Al_2O_3/TiO_2 ratios that are generally lower than 12 (Fig. 5b), plot in the high-Fe basalt field of the Jensen's (1976) cations ternary diagram (Fig. 5e), and have a transitional magmatic affinity. Chondrite-normalized REEs of the mafic units show a flat pattern, with values ranging between 10 and 30 times that of chondrite (Fig. 6c).

The ultramafic rocks have Al_2O_3/TiO_2 ratios that are higher than 12 (Fig. 5b), plot in the peridotitic to basaltic komatiite field of the Jensen's cations ternary diagram (Fig. 5e), and their magmatic affinity is tholeiitic to transitional (Fig. 5d). Four different signatures of ultramafic units can be recognized (5a, 5b, 5c, 5d). Chondrite-normalized REE plots for the 5a, 5b, and 5c subunits show slight depletions or slight enrichments in LREEs relative to HREEs (Fig. 6d). The LREE values vary considerably, between 1.5 to 20 times those of chondrite. Subunit 5d analyses plot in the basaltic komatiite field of the Jensen's cations ternary diagram (Fig. 5e). It has higher REE values, but similar pattern to unit 5c with depleted LREEs relative to the HREEs (Fig. 6c, d).

Minor rock types

A minor mafic rock type (unit 6) occurs as a layer in the quartzite (Fig. 3). This unit has the same signature as the mafic rocks of unit 4, with Al_2O_3/TiO_2 ratios lower than 12 (Fig. 5b). Unit 6 analyses lie in the high-Fe basalt field of the Jensen's cations ternary diagram (Fig. 5e) and have a transitional magmatic affinity. Chondrite-normalized REE values show a flat pattern similar to that of unit 4 (Fig. 6c).

Unit 7 also occurs as a layer within the quartzite (Fig. 3, 4). It has a signature similar to the intermediate subunit 1a, although unit 7 generally lacks the Zr-Hf positive anomalies and has a higher Th content (Fig. 6e).

Unit 8 consists of intermediate dykes that are intersected in drill core and visible along the western wall of pit E (Fig. 3, 8a). The signature of this unit is similar to that of the intermediate to felsic subunits 2a and 2c (Fig. 5, 6f). Chondrite-normalized trace and REE plots of unit 8 show a slight depletion in HREEs, but generally a higher LREE signature than that of subunit 2c.

A minor felsic rock, unit 3, is locally present in drill cores, but its sporadic occurrence and distribution do not allow for correlations across interpreted sections. The geochemical signature of unit 3 is distinct from that of the other units at Meadowbank mine with much higher Zr/TiO_2 and Al_2O_3/TiO_2 ratios (Fig. 5b). Unit 3 has a rhyodacitic to rhyolitic composition (Fig. 5c) and a calc-alkaline affinity (Fig. 5d). Chondrite-normalized trace and REE plots for this unit show variable patterns with a moderate negative slope, a negative Zr anomaly and a strong negative Ti anomaly (Fig. 6g).

STRUCTURE

The Meadowbank deposit is strongly deformed. Numerous folds and faults are present in the open pit area and six generations of structures have been delineated on the basis of structural style, orientation, and crosscutting relationship and are described below in apparent chronological order. 1) Along the east wall of Portage open pit (Fig. 3), a penetrative bedding- and/or layering-parallel schistosity, S_{P1}, is generally south-trending and dips shallowly to moderately (about 30°) to the west (Fig. 8b). S_{P1} is regionally associated with isoclinal folds (Proterozoic F_{P1} of Pehrsson et al. (2013)), only one of which have been recognized at the mine scale. 2) A series of early fault zones occur in the Portage open pit. Some are delineated by ultramafic rocks whereas others cause the duplication of volcaniclastic rocks and quartzite with the development of fault-bounded panels (Fig. 3b, 4, 7). So far, no reliable kinematic indicators for these fault zones have been identified; however, based on the interpreted section 7025 (Fig. 4), the fault zones are apparently east directed. The relative timing of such fault zones is difficult to determine, but they are clearly folded and faulted by D_{P2} structures and are therefore termed D_{P1} fault zones (Fig. 3, 4, 7). 3) Tight to isoclinal F_{P2} folds with subhorizontal south-trending axes occur in southeast part of the Portage open pit (push back area; Fig. 3, 7b, 8c) and eastward, where they fold mineralized banded iron-formation units and intermediate to felsic rocks (Fig. 7a). F_{P2} folds have an apparent eastward vergence that contrasts with the regional northwest vergence of F_{P2} folds (Pehrsson et al., 2013). Mesoscopic isoclinal folds and axial-planar S_{P2} foliation are locally present although the S_{P2} fabric is rarely penetrative in hinge zones of folds affecting banded iron-formation units. Along the limbs of F_{P2} folds, S_{P2} is coplanar to the S_{P1} schistosity, forming a composite S_{P1-2} fabric (Fig. 9a). 4) Several late D_{P2} fault zones are also outlined by ultramafic rocks (Fig. 3, 4, 7, 8c, d, e), and some of which may have reactivated D_{P1} faults (Fig. 7). Two subparallel late D_{P2} fault zones (termed

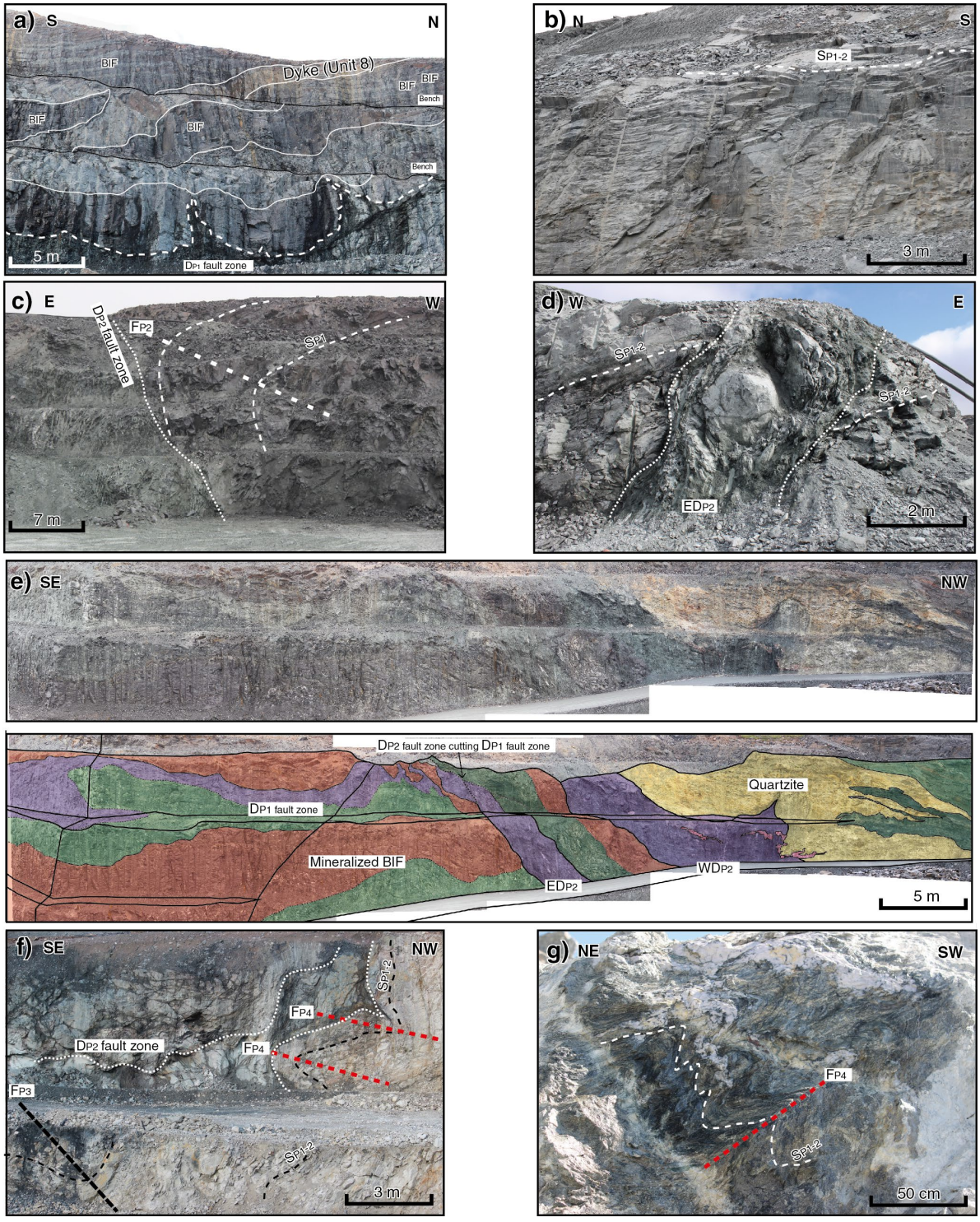

Figure 8. Representative photographs illustrating the structural geology of the Meadowbank deposit. **a)** D_{P1} fault zone subconcordant to the mine sequence and intermediate dyke cutting banded iron-formation (BIF) (west wall, pit E); 2014-197; **b)** composite S_{P1-2} fabric in intermediate to felsic volcaniclastic rocks; 2014-198; **c)** F_{P2} fold truncated by a D_{P2} fault zone (in ultramafic rocks), interpreted as inherited from a D_{P1} structure (push back area); 2014-190; **d)** D_{P2} fault zone in ultramafic rocks cutting the composite fabric S_{P1-2} in the volcaniclastic rocks (pit D); 2014-183; **e)** western and eastern D_{P2} fault zones (WDP2 and EDP2, respectively) marked by ultramafic rocks, the eastern fault zone cuts a D_{P1} fault zone and mineralized banded iron-formation along its footwall (pit E, south ramp); 2014-191; **f)** F_{P3} and F_{P4} folds (mine-scale nomenclature) outlined by quartzite and a D_{P2} fault zone (pit A, west wall); 2014-187; **g)** strongly foliated (S_{P1-2}) sericite schist deformed by southwest-verging F_{P4} folds (mine-scale nomenclature; pit A, west wall); 2014-196. All photographs by V. Janvier.

herein the western fault zone (WD_{P2}), and eastern fault zone (ED_{P2}); Fig. 8d, e) are recognized along the western wall of the Portage open pit (Fig. 3). Both cut earlier structures and ore zones, but are affected by F_{P3} and F_{P4} folds (Fig. 3, 7, 8e). Although kinematic indicators are rare in volcanic units, some in sheared ultramafic rocks suggest a down-to-the-west relative motion. These two late phases of folding are mapped in the mine area, but their correlations with the regional D_{P3} and D_{P4} folding events (e.g. Pehrsson et al., 2013) are still unclear as their crosscutting relationships appear to be contradictory. At deposit scale, the relative timing of these late folding events is inverted so that F_{P3} and F_{P4} folds correspond respectively with the regional F_{P4} and F_{P3} folds. These two folding events are differentiated by their vergence and wavelength. 5) In North Portage (pit A; Fig. 3, 8f), the mine sequence turns abruptly to the west, affected by a shallow southwest-plunging, southeast-verging megascopic F_{P3} chevron-style synform (Fig. 3, 8f). Southward,

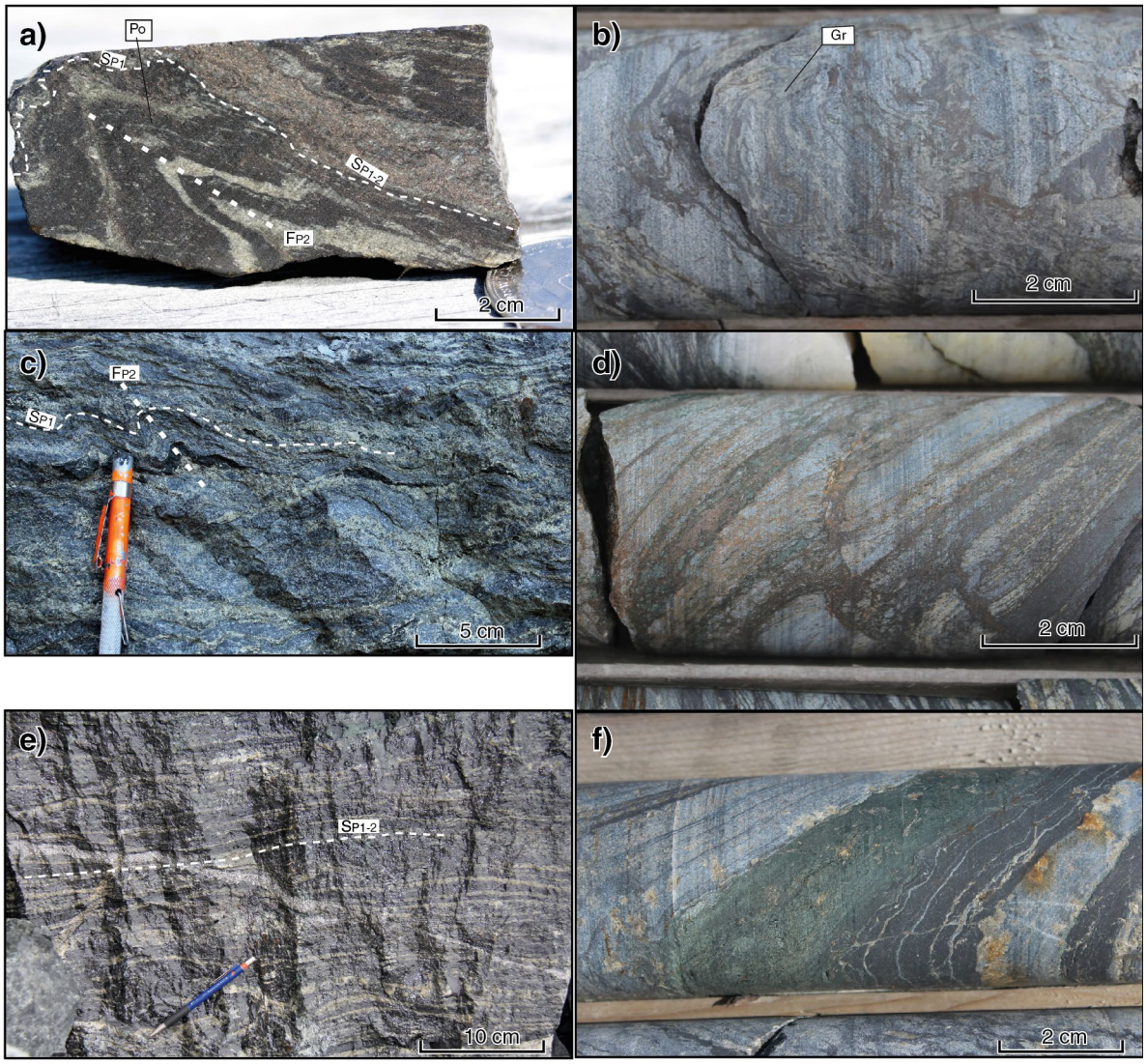

Figure 9. Representative photographs of mineralized and barren banded iron-formation units with associated mineral assemblages of the Meadowbank deposit. **a)** Mineralized and strongly deformed banded iron-formation; note thin disseminated grunerite (Gr) where pyrrhotite (Po) replaces magnetite; photograph by P. Mercier-Langevin; 2014-195; **b)** banded iron-formation with pyrrhotite replacing magnetite layers along the S_{P1} fabric and remobilized in the F_{P2} fold limbs; photograph by V. Janvier; 2014-188; **c)** mineralized banded iron-formation with pyrrhotite replacing magnetite in folded fabric S_{P1} and remobilized along transposed F_{P2} limb; photograph by V. Janvier; 2014-185; **d)** transposed pyrrhotite and pyrite stockwork in banded iron-formation–chert layers with minor pervasive chlorite alteration; photograph by V. Janvier; 2014-184; **e)** arsenopyrite vein (arrow) cutting the banded iron-formation layering, both affected by the S_{P1-2} fabric; photograph by V. Janvier; 2014-193; **f)** barren banded iron-formation with chlorite bands and porphyroblastic acicular grunerite; photograph by V. Janvier; 2014-186

along the long limb of this megascopic fold, minor F_{P3} folds occur in the Portage pit B and Goose open pit, where they produce slight undulations of the lithological contacts and main fabric (Fig. 3, 4, 7b). No axial-planar fabric S_{P3} has been mapped thus far in the mine area. 6) The last folding phase D_{P4} is characterized by mesoscopic shallowly- to moderately-inclined, open to tight folds with a south-southwest vergence (Fig. 8f, g). A conspicuous axial-planar crenulation cleavage S_{P4} is roughly northwest-trending and dips northward between 10 to 45°. The dip and orientation of the cleavage are constant and apparently not folded, so that, at the mine scale, the relative timing of D_{P4} deformation is interpreted as the youngest folding phase.

ORE ZONES: MINERAL ASSEMBLAGES AND DISTRIBUTION

The bulk of the gold at Meadowbank mine is hosted in Algoma-type (Gross, 1980), banded magnetite-chert iron-formation units. The typical mineralized banded iron-formation is generally intensely deformed, rich in sulphide minerals, mainly pyrrhotite±pyrite as the main ore-related minerals, with traces of chalcopyrite and arsenopyrite. Grunerite is common in chert bands (Fig. 9a, b). In general, the ore occurs as pyrrhotite and/or pyrite replacements of magnetite bands (Fig. 9a, b, c), but pyrrhotite and pyrite are also found in high-strain zones (Fig. 9a) or as a transposed stockwork in magnetite and chert bands accompanied by local pervasive chlorite alteration (Fig. 9d). The best gold intersections are often intensely deformed and primary layering in the units is transposed or disrupted, forming dismembered masses of quartz, pyrrhotite, and relict magnetite (Fig. 9a, b). Despite a nonlinear correlation between sulphide minerals (pyrrhotite) and gold, the presence of pyrrhotite and/or pyrite usually indicates the likelihood of good gold grades. Barren banded iron-formation units are usually much less deformed, and bedding is preserved, although the presence of chlorite-rich layers and porphyroblastic acicular grunerite is typical (Fig. 9f). Another style of mineralization consists of gold-bearing quartz-pyrrhotite±pyrite veins hosted in intermediate to felsic volcaniclastic rocks, locally forming spectacular high-grade ore (Fig. 10a). These veins are transposed and/or sheared (C: shear plane) and boudinaged (C′: synthetic riedel or secondary shear plane) into the composite S_{P1-2} schistosity and are affected by a younger fabric (S_{P4}: Fig. 10a, b). The presence of kinematically compatible sigmoidal boudinaged quartz veins are in agreement with an apparent eastward motion on D_{P1} fault zones (Fig. 4). In terms of alteration, disseminated pyrite commonly occurs in the selvages of these veins (Fig. 10b), whereas chlorite and sericite form a metre-scale alteration halo around the veins. Based on the alteration boxplot diagram (Fig. 10c) and drill-core observations (Fig. 10d), sericite overprints chlorite. In addition, rare carbonate is also present in altered volcaniclastic rocks. Besides some disseminated calcite in subunit 1c, there is no carbonate alteration associated with the Portage and Goose deposits. Iron carbonate alteration is, however, common in the region and well developed at the Vault gold deposit approximately 10 km north of the Portage deposit (Dupuis et al., 2014). The greenschist to amphibolite facies transition, although gradual along the length of the deposit, is located between the Portage and Goose deposits (Pehrsson et al., 2004; Sherlock et al., 2004). The mineral assemblages associated with the ore gradually change southward where biotite, Fe-Mg amphibole, and garnet occur in variable proportions, replacing chlorite and sericite as the main alteration-related minerals.

There are important spatial relationships between the ore zones and the main structural features of the deposit. The authors' mapping and preliminary interpretations indicate that gold is spatially associated with some of the earliest structures observed at Portage and Goose deposits. In pit E, the ore zones are exclusively hosted in iron-formation occurring between sheared ultramafic rocks (hanging wall), and intermediate volcaniclastic rocks (footwall), both contacts marked by folded D_{P1} fault zones (Fig. 7). To the north in pits A, B, C, and D, gold mineralization is also hosted in part by volcaniclastic rocks and occurs in zones, frequently concordant to lithological contacts that are interpreted as D_{P1} fault zones (Fig. 4). The concentration of sulphide minerals along sheared F_{P2} fold limbs (Fig. 9a) suggests that part of the ore distribution is controlled by D_{P2}, either as a local remobilization or as a distinct early- to syn-D_{P2} mineralization. Late Granoblastic arsenopyrite veins that truncate the layering are affected by the S_{P1-2} fabrics, which also suggest a pre- to early D_{P2} mineralizing event (Fig. 9e). Ongoing work at Meadowbank mine aims at refining the relative and absolute timing between generations of structures and hydrothermal activity in order to better constrain the main mineralizing processes; however, based on the authors' observations, chemical (banded iron-formation) and structural traps (D_{P1} and D_{P2} fault zones, and F_{P2} folds) have clearly exerted a control on ore distribution.

DISCUSSION

Before this study, the lithostratigraphy of the Meadowbank mine area was divided into four main volcanic units including intermediate, intermediate to felsic, mafic, and ultramafic rocks (Armitage et al., 1996; Hrabi et al., 2003; Sherlock et al., 2004). The analysis of the 'immobile elements' has allowed for the identification of several distinctive subunits including three intermediate subunits (i.e. 1a, 1b, 1c), three intermediate to felsic subunits (i.e. 2a, 2b, 2c), one felsic unit (i.e. 3), one mafic unit (i.e. 4), and four ultramafic subunits (i.e. 5a, 5b, 5c, 5d). This detailed subdivision has helped to better define the structural and lithostratigraphic settings of the Portage and Goose deposits. Subtle geochemical variations among subunits can be due to a combination of processes such as alteration, crustal contamination or assimilation, fractional crystallization, and magma mixing, among others (e.g. Sparks, 1986; Nicholson

et al., 1991; Reiners et al., 1995). Preliminary interpretation of the data suggests that the geochemical variations of the Meadowbank mine host rocks are due to primary processes that were partially obscured by superimposed alteration and metamorphism. Elemental ratios such as Nb/Th, Ta/La (proxy for subduction-related contamination), and Sc/Yb (proxy for magmatic differentiation) can be used to determine which phenomenon is responsible for the primary geochemical variations. For example, chondrite-normalized trace and REE plots allow the discrimination of two signatures for the intermediate subunits 1a and 1c (Fig. 6a). The highest chondritic value in Th for subunit 1a can be explained by increased crustal contamination or assimilation (Pearce, 2008). Here, the pronounced negative Nb, Ta, and

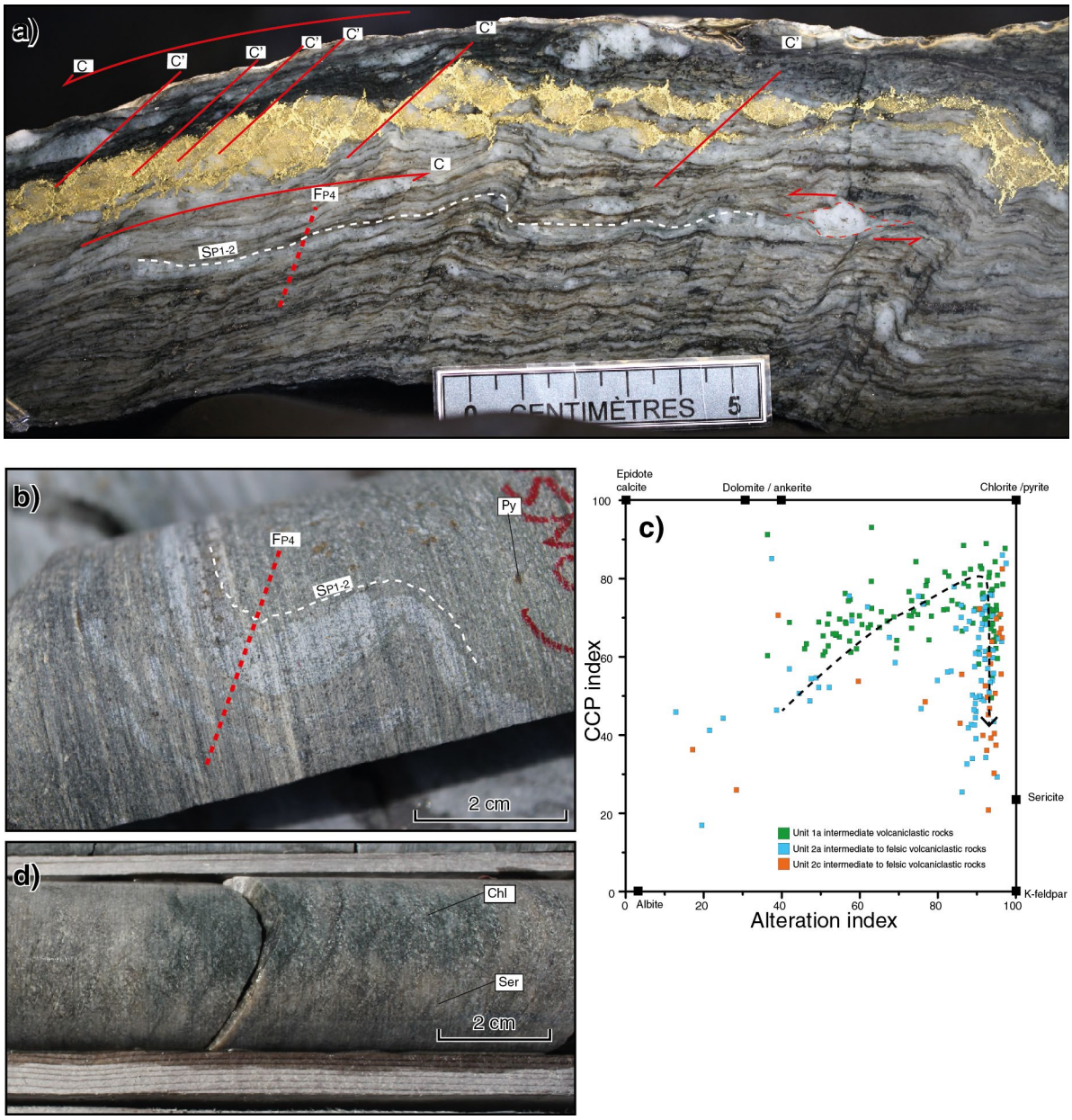

Figure 10. Representative photographs of mineralized and barren volcaniclastic rocks with associated mineral assemblages of the Meadowbank deposit. **a)** Felsic schist showing the dominant composite S_{P1-2} fabric and transposed and/or boudinaged gold quartz veins, affected by the S_{P4} crenulation cleavage (mine-scale structural nomenclature); photograph by P. Mercier-Langevin; 2014-192; **b)** Intermediate to felsic volcaniclastic rock with a pyrite-chlorite-sericite assemblage adjacent to a gold-quartz vein deformed by F_{P4} asymmetric folding; photograph by V. Janvier; 2014-194; **c)** Al-CCPI alteration box plot illustrating chlorite and pyrite alteration followed by muscovite alteration; Al (Ishikawa alteration index): $100(MgO+K_2O)/(MgO+K_2O+CaO+Na_2O)$; CCPI (chlorite-carbonate-pyrite index): $100(FeO+MgO)/(FeO+MgO+Na_2O+K_2O)$ (*modified from* Large et al., 2001); **d)** Barren intermediate to felsic volcaniclastic rock with a chlorite-sericite assemblage; sericite (Ser) is overprinting chlorite (Chl); photograph by V. Janvier; 2014-194

Ti anomalies, common to all intermediate to felsic volcanic rocks, suggest an arc-like affinity. Obviously, more work is necessary to get a clear picture of the petrogenetic evolution of the Portage and Goose host rocks and the geodynamic setting in which they were generated, but preliminary assessment shows that these rocks are comparable to a number of other greenstone belts of similar age (Corfu et al., 1989). More importantly, the mine-scale protoliths defined herein nicely correlate with those defined regionally (Zaleski et al., 1999b; Pehrsson et al., 2013), despite the use of different data sets. As such, regional protolith determination can be used as a regional exploration tool to better outline the specific prospective stratigraphic horizons and key geological structures.

Based on the authors' observations, major structures clearly control the location and geometry of the ore at Meadowbank mine, which can be categorized as an epigenetic banded iron-formation–hosted gold deposit. The presence of F_{P2} folds (e.g. push back area; Fig. 7b) and the repetition of several horizons by D_{P1} and possibly late D_{P2} fault zones (Fig. 4) are major structural features controlling the geometry of ore zones. The distribution of gold mineralization in the Portage deposit apparently follows two trends (section 7025; Fig. 4). These trends are slightly discordant to the lithological contacts and locally coincide with truncations of units, and are thus interpreted as marking discrete D_{P1} faults. Similarly southward, along sections 5775 and 6175 (Fig. 7), the bulk of the gold mineralization occurs below the contact between banded iron-formation units and ultramafic rocks, which delineates the footwall of a D_{P1} fault zone.

Establishing the relationships and controls between structural geology and gold mineralization is a key aspect of the present study. Previous research (e.g. Armitage et al., 1996; Sherlock et al., 2004) has proposed that gold was introduced during the regional D_{P2} deformation at around 1.83 Ga. The present authors propose that gold mineralization occurred prior to, or very early during D_{P2} based on the following: 1) the occurrence of transposed-boudinaged (remobilized) high-grade gold-quartz veins into the composite S_{P1-2} foliation (Fig. 10a) suggests that gold-quartz veins were introduced either during D_{P1} or early during D_{P2}; 2) The presence of D_{P2} fault zones that crosscut the S_{P1-2} composite fabric (Fig. 8d, e); 3) the replacement of S_{P1}-foliated magnetite layers (S_0) by pyrrhotite, which are folded by F_{P2} (Fig. 9a, c); 4) the spatial association of gold with D_{P1} fault zones (Fig. 4, 7), which are folded by F_{P2} folds (Fig. 7a); and 5) a preliminary Re-Os age of ca. 1899 Ma (R. Creaser, pers. comm., 2013) on an auriferous arsenopyrite vein affected by S_{P1-2}, which is contemporaneous with the older published regional age constraints for D_{P1} and D_{P2} (i.e. 1.91–1.83 Ga; Pehrsson et al. (2013)).

CONCLUSION

Access to mine workings, new outcrops, exploration and delineation drilling, and mining data coupled with an in-depth geochemical characterization of the Meadowbank deposit host rocks brings a wealth of new and key information on the lithostratigraphic setting and structural evolution that led to the formation of the deposit and its current geometry. Lithogeochemistry is an essential tool to help distinguish and map the polydeformed volcanic rocks that host the Meadowbank gold deposit. A better control on the distribution of units and subunits hosting the deposit helps to better define its very complex geometry and delineate major structural features that were previously unrecognized at mine scale. The lithogeochemical data set is also being used to better characterize the alteration associated with the ore zones and overall footprint. Now that the knowledge of primary composition of the host units has been improved, the study will focus on the hydrothermal alteration associated with the mineralizing event(s).

The bulk of the gold mineralization at Meadowbank mine is associated with pyrrhotite, grunerite, and minor chlorite, and hosted in strongly deformed banded iron-formation in sheared or faulted contacts with ultramafic rocks. A significant amount of the gold also occurs in quartz veins in adjacent volcaniclastic rocks, in association with disseminated pyrite, chlorite, and sericite. Carbonate alteration is not significant at Meadowbank mine compared to other banded iron-formation–hosted Au deposits and other prospects in the Meadowbank deposit area (Dupuis et al., 2014).

Polyphase folding and faulting resulted in a complexly deformed deposit. Nevertheless, crosscutting relationships and preliminary Re-Os dating suggest that gold mineralization occurred prior to the peak of D_{P2} deformation. Here, the authors propose that the D_{P1} fault zones have played a major control on the actual ore distribution and probably genesis of the deposit. Ongoing work at Meadowbank mine aims at better constraining the age of the ore-forming events and the geochemical and mineralogical signatures of the gold-bearing hydrothermal event(s).

ACKNOWLEDGMENTS

This contribution emanated mainly from the Ph.D. thesis research of V. Janvier at the Institut National de la Recherche Scientifique (INRS-ETE), as part of the Targeted Geoscience Initiative 4 (Lode Gold project) of Natural Resources Canada. The authors thank Agnico Eagle Mines Ltd. for access to the property, drill cores, and various databases, and for chartered transport and accommodation. The staff of the AEM Meadowbank and Exploration divisions are acknowledged for their time, support, and interest in this project. F. Béland provided very helpful field assistance. The authors are grateful to N. Pinet (GSC Quebec) for his review of the manuscript.

REFERENCES

Armitage, A.E. and James, R.S., 1991. Geology of the Third Portage Lake area, north of Baker Lake, District of Keewatin, NWT; Indian and Northern Affairs Canada, EGS 1990-14, p. 17.

Armitage, A.E., James, R.S., and Goff, S.P., 1996. Gold mineralization in Archean banded iron formation, Third Portage Lake area, Northwest Territories, Canada; Exploration and Mining Geology, v. 5, p. 1–15.

Ashton, K.E., 1988. Precambrian geology of the southeastern Amer Lake area (66H/1), near Baker Lake, N.W.T.; a study of the Woodburn Lake Group, an Archean orthoquartzite-bearing sequence in the Churchill structural province; Ph.D. thesis, Queen's University, Kingston, Ontario, 335 p.

Barrett, T.J. and MacLean, W.H., 1999. Volcanic sequences, lithogeochemistry, and hydrothermal alteration in some bimodal volcanic-associated massive sulfide systems; Reviews in Economic Geology, v. 8, p. 101–131.

Berman, R.G., Sanborn-Barrie, M., Stern, R.A., and Carson, C.J., 2005. Tectonometamorphism at ca. 2.35 and 1.85 Ga in the Rae domain, western Churchill Province, Nunavut, Canada: insights from structural, metamorphic and in situ geochronological analysis of the southwestern Committee Bay belt; Canadian Mineralogist, v. 43, p. 409–442. doi:10.2113/gscanmin.43.1.409

Berman, R.G., Davis, W.J., and Pehrsson, S., 2007. Collisional Snowbird tectonic zone resurrected: growth of Laurentia during the 1.9 Ga accretionary phase of the Hudsonian orogeny; Geology, v. 35, p. 911–914. doi:10.1130/G23771A.1

Castonguay, S., Janvier, V., Mercier-Langevin, P., Dubé, B., McNicoll, V., Malo, M., Pehrsson, S., and Bécu, V., 2012. Recognizing optimum banded-iron formation-hosted gold environments in ancient, deformed and metamorphosed terranes: preliminary results from the Meadowbank deposit, Nunavut; *in* Abstracts Volume, 40th Annual Yellowknife Geoscience Forum, (comp.) D.M. Watson; Yellowknife, Northwest Territories, November 13–15, p. 54.

Castonguay, S., Janvier, V., Mercier-Langevin, P., Dubé, B., McNicoll, V., Malo, M., Pehrsson, S., and Bécu, V., 2013. Recognizing optimum banded iron formation (BIF)-hosted gold environments: preliminary results from the Meadowbank deposit; 2013 Nunavut Mining Symposium; Iqaluit, Nunavut, April 9–11, 2013. <http://2013.nunavutminingsymposium.ca/wp-content/uploads/2013/04/2-Castonguay-GSC.pdf> [accessed October 1, 2014]

Corfu, F., Krogh, T.E., Kwok, Y.Y., and Jensen, L.S., 1989. U-Pb zircon geochronology in the southwestern Abitibi greenstone belt, Superior Province; Canadian Journal of Earth Sciences, v. 26, p. 1747–1763. doi:10.1139/e89-148

Dubé, B., Mercier-Langevin, P., Castonguay, S., McNicoll, V.J., Pehrsson, S.J., Bleeker, W., Schetselaar, E.M., and Jackson, S., 2011. Targeted Geoscience Initiative 4. Lode gold deposit in ancient, deformed and metamorphosed terranes — footprints and exploration implications: a preliminary overview of themes, objectives and targeted areas; *in* Summary of Field Work and Other Activities 2011; Ontario Geological Survey, Open File Report 6270, p. 38.1–38.10.

Dupuis, C., Mercier-Langevin, P., and McNicoll, V., Janvier, V., Dubé, B., Castonguay, S., de Chavigny, B., Pehrsson, S., and Côté-Mantha, O., 2014. The Vault gold deposit, Meadowbank area, Nunavut: preliminary results on the nature and timing of mineralization; *in* Abstracts Volume; Geological Association of Canada–Mineralogical Association of Canada annual joint meeting, Fredericton, New Brunswick, May 21–23, 2014, v. 37, p. 81.

Gourcerol, B., Thurston, P.C., Kontak, D.J., and Côté-Mantha, O., 2014. Interpretations and implications of preliminary LA ICP-MS analysis of chert for the origin of geochemical signatures in banded iron-formations (BIFs) from the Meadowbank gold deposit, western Churchill Province, Nunavut; Geological Survey of Canada, Current Research 2014-1, 22 p. doi:10.4095/293129

Gross, G.A., 1980. A classification of iron formations based on depositional environments; Canadian Mineralogist, v. 18, p. 215–222.

Henderson, J.R., Henderson, M.N., Pryer, L.L., and Cresswell, R.G., 1991. Geology of the Whitehills-Tehek area, District of Keewatin: an Archean supracrustal belt with iron formation-hosted gold mineralization in the central Churchill Province; *in* Current Research, Part C; Geological Survey of Canada, Paper 91-1C, p. 149–156.

Hoffman, P.F., 1989. Precambrian geology and tectonic history of North America; *in* The Geology of North America – An Overview; Geological Society of America, The Geology of North America, Part A, p. 447–512.

Hrabi, R.B., Barclay, W.A., Fleming, D., and Alexander, R.B., 2003. Structural evolution of the Woodburn Lake group in the area of the Meadowbank gold deposit, Nunavut; Geological Survey of Canada, Current Research 2003-C27, 10 p. doi:10.4095/214396

Janvier, V., Castonguay, S., Mercier-Langevin, P., Dubé, B., McNicoll, V., Malo, M., Pehrsson, S.J., and Bécu, V., 2013. Recognizing optimum banded-iron formation-hosted gold environments in ancient, deformed and metamorphosed terranes: preliminary results from the Meadowbank deposit, Nunavut, Canada; Geological Survey of Canada, Open File 7407, 1 sheet. doi:10.4095/292589

Jensen, L.S., 1976. A new cation plot for classifying subalcalic volcanic rocks; Ontario Division of Mines, Miscellaneous Paper 66, 21 p.

Large, R.R., Gemmell, J.B., Paulick, H., and Huston, D.L., 2001. The alteration box plot: a simple approach to understanding the relationship between alteration mineralogy and lithogeochemistry associated with volcanic-hosted massive sulfide deposits; Economic Geology and the Bulletin of the Society of Economic Geologists, v. 96, p. 957–971.

McDonough, W.F. and Sun, S.-S., 1995. The composition of the Earth; Chemical Geology, v. 120, p. 223–253. doi:10.1016/0009-2541(94)00140-4

Nicholson, H., Condomines, M., Fitton, J.G., Fallick, A.E., Grönvold, K., and Rogers, G., 1991. Geochemical and isotopic evidence for crustal assimilation beneath Krafla, Iceland; Journal of Petrology, v. 32, p. 1005–1020. doi:10.1093/petrology/32.5.1005

Pearce, J.A., 2008. Geochemical fingerprinting of oceanic basalts with applications to ophiolite classification and the search for Archean oceanic crust; Lithos, v. 100, p. 14–48. doi:10.1016/j.lithos.2007.06.016

Pehrsson, S.J., Wilkinson, L., and Zaleski, E., 2004. Geology, Meadowbank gold deposit area, Nunavut; Geological Survey of Canada, Open File 4269, scale 1: 20 000. doi:10.4095/215550

Pehrsson, S.J., Berman, R.G., and Davis, W.J., 2013. Paleoproterozoic orogenesis during Nuna aggregation: a case study of reworking of the Rae craton, Woodburn Lake, Nunavut; Precambrian Research, v. 232, p. 167–188. doi:10.1016/j.precamres.2013.02.010

Reiners, P.W., Nelson, B.K., and Ghiorso, M.S., 1995. Assimilation of felsic crust by basaltic magma: thermal limits and extents of crustal contamination of mantle-derived magmas; Geology, v. 23, p. 563–566. doi:10.1130/0091-7613(1995)023<0563:AOFCBB>2.3.CO;2

Sherlock, R.L., Alexander, R.B., March, R., Kellner, J., and Barclay, W.A., 2001a. Geological setting of the Meadowbank iron-formation-hosted gold deposits, Nunavut; Geological Survey of Canada, Current Research 2001-C11, 23 p. doi:10.4095/212081

Sherlock, R., Alexander, B., March, R., and Kellner, J., 2001b. Geology of the Meadowbank iron formation hosted gold deposits; Geological Survey of Canada, Open File 3149, scale 1:7500. doi:10.4095/212961

Sherlock, R., Pehrsson, S.J., Logan, A.V., Hrabi, R.B., and Davis, W.J., 2004. Geological setting of the Meadowbank gold deposits, Woodburn Lake Group, Nunavut; Exploration and Mining Geology, v. 13, p. 67–107. doi:10.2113/gsemg.13.1-4.67

Skulski, T., Sandeman, H., Sandborn-Barrie, M., MacHattie, T., Young, M., Carson, C., Berman, R., Brown, N., Rayner, D., Pangapko, D., Byrne, D., and Deyell, C., 2003. Bedrock geology of the Ellice Hills map area and new constraints on the regional geology of the Committee Bay area, Nunavut; Geological Survey of Canada, Current Research 2003-C22, 11 p. doi:10.4095/214204

Sparks, R.S.J., 1986. The role of crustal contamination in magma evolution through geological time; Earth and Planetary Science Letters, v. 78, p. 211–223. doi:10.1016/0012-821X(86)90062-2

Winchester, J.A. and Floyd, P.A., 1977. Geochemical discrimination of different magma series and their differentiation products using immobile elements; Chemical Geology, v. 20, p. 325–343. doi:10.1016/0009-2541(77)90057-2

Zaleski, E. and Pehrsson, S., 2005. Geology, Half Way Hills and Whitehills Lake area, Nunavut; Geological Survey of Canada, Map 2069A, scale 1:50 000. doi:10.4095/220576

Zaleski, E., Henderson, J.R., Corrigan, D., Jenner, G.A., Kjarsgaard, B.A., and Kerswill, J.A., 1997. Preliminary results of mapping and structural interpretation from the Woodburn project, western Churchill province, Northwest Territories; *in* 1996 Exploration Overview, (ed.) S. Goff and K. Gochnauer; Northwest Territories Geoscience Office, p. 3.43–3.44.

Zaleski, E., Duke, N., L'Heureux, R., and Wilkinson, L., 1999a. Geology, Woodburn Lake group, Amarulik Lake to Tehek Lake, Kivalliq Region, Nunavut; Geological Survey of Canada, Open File 3743, scale 1:50 000. doi:10.4095/210634

Zaleski, E., L'Heureux, R., Duke, N., Wilkinson, L., and Davis, W.J., 1999b. Komatiites and felsic volcanic rocks overlain by quartzite, Woodburn Lake group, Meadowbank River area, Western Churchill Province, Northwest Territories (Nunavut); *in* Current Research 1999-C; Geological Survey of Canada, p. 9–18.

Zaleski, E., Davis, W.J., and Sandeman, H.A., 2001. Continental extension, mantle magmas & basement/cover relationships; *in* Extended Abstracts Volume, Fourth International Archaean Symposium, Perth, Australia, September 24–28, 2001, p. 374–376.

Geological Survey of Canada Project 340331NU61